Toxicology Letters 266 (2017) 65–73

Contents lists available at ScienceDirect

Toxicology Letters

journal homepage: www.elsevier.com/locate/toxlet

Full Length Article

Immunotoxicological effects of arsenic bioaccumulation on spatial metallomics and cellular enzyme response in the spleen of male Wistar rats after oral intake

Elio A. Soria[a,*], Roberto D. Pérez[b], Ignasi Queralt[c], Carlos A. Pérez[d], Guillermina A. Bongiovanni[e]

[a] Instituto de Investigaciones en Ciencias de la Salud (INICSA), Universidad Nacional de Córdoba, CONICET, FCM, Córdoba, Argentina
[b] Instituto de Física Enrique Gaviola (IFEG), Universidad Nacional de Córdoba, CONICET, FAMAF, Córdoba, Argentina
[c] Institute of Environmental Assessment and Water Research (IDAEA), CSIC, Barcelona, Spain
[d] Laboratório Nacional de Luz Síncrotron (LNLS), CNPEM, Campinas, Brazil
[e] Instituto de Investigación y Desarrollo en Ingeniería de Procesos, Biotecnología y Energías Alternativas (PROBIEN), Universidad Nacional del Comahue, CONICET, FCA, Neuquén, Argentina

HIGHLIGHTS

- Arsenic is immunotoxic and accumulated in the spleen tissues.
- Arsenic causes spatial disturbances of metals in the spleen tissues.
- Arsenic modifies the activity of redox enzymes in splenocytes.
- Arsenic, metals, redox enzymes and spleen tissues are related.

ARTICLE INFO

Article history:
Received 30 May 2016
Received in revised form 15 December 2016
Accepted 18 December 2016
Available online 19 December 2016

Keywords:
Immunodeficiency
Oxidative stress
Sodium arsenite
X-ray fluorescence spectrometry

ABSTRACT

Arsenic (As) is a worldwide environmental contaminant, which compromises immunity and causes various associated disorders. To further investigate its immunotoxicity, male Wistar rats were exposed to 100 ppm of sodium arsenite (inorganic AsIII) in drinking water for 2 months. Given that metals are signi ficant immune regulators, their content and distribution were analysed in spleen tissues, to then evaluate subsequent changes of redox enzyme responses in spleen parenchyma cells (splenocytes). X-ray fluorescence spectrometry demonstrated As accumulation in both white and red pulps ($p < 0.005$), and As-related pulp-dependent modifications of the content of Cu, Ca, Zn and Fe ($p < 0.01$). Correlational path analysis revealed direct effects of As on their spatial distribution (Cu: −0.76, Ca: −0.61, Zn: 0.38; $p < 0.02$). As-exposed splenocytes showed γ-glutamyltranspeptidase inhibition, peroxidase induction, and variable responses of nitric oxide synthase ($p < 0.05$). Concanavalin A-treated splenocytes (T cell mitogen) were more susceptible *in vitro* to these As-related enzymatic changes than those treated with lipopolysaccharide (B cell mitogen) ($p < 0.05$). The study thus established the impact of As bioaccumulation on metallic spatial homeostasis in the spleen, and then identified enzymatic dysfunctions in splenocytes. This suggested that arsenic disrupts biometal-dependent immune pathways and redox homeostasis, with mitogen exposure modifying the toxicological response.

1. Introduction

Arsenic (As) is a toxic metalloid that is widely present in the environment (20th element in the Earth's crust) and in the human body (12th element) (Jomova et al., 2011). Non-occupational human exposure is mainly by ingestion of contaminated food and

* Corresponding author at: INICSA, Enrique Barros, Córdoba 5014, Argentina.
E-mail address: easoria@fcm.unc.edu.ar (E.A. Soria).

http://dx.doi.org/10.1016/j.toxlet.2016.12.014
0378-4274/

drinking water. Groundwater contamination is known in 35 countries, with more than 130 million people in Asia and 14 million in Latin America being exposed (Bundschuh et al., 2012; Chakraborti and Nriagu, 2011).

Chronic exposure to arsenic causes, among others, skin lesions, vascular disorders, metabolic pathologies, neuropathies, nephropathies and many types of cancer (Grasso et al., 2011; Paul et al., 2013). Although these diseases are well-recognised, their molecular mechanisms need further study. Several hypotheses have been suggested about As-induced pathology (Hong et al., 2014), including overproduction of reactive oxygen species (ROS) and reactive nitrogen species (RNS) (Ray et al., 2014; Sharma et al., 2014). Arsenic also induces immune dysfunctions, such as chronic inflammation, autoimmunity, and immunodeficiency with opportunistic illnesses (Schulz et al., 2002; Tarantino et al., 2013). However, its specific immune effects remain only partly understood.

After intake, As is well absorbed in rats, reaching the bloodstream and binding to erythrocytes (Biswas et al., 2008). Rats exhibit a unique haemoglobin alpha chain with a cysteine residue, which strongly binds and retains trivalent As (Lu et al., 2007). It then deposits in the liver, kidneys, lungs, skin, and spleen (Cui and Okayasu, 2008; McClintock et al., 2012; Rubatto Birri et al., 2010), targeting lymphocytes (Ullah et al., 2015). The spleen has two areas (white lymphocyte-enriched pulp, and red erythrocyte-enriched pulp with macrophages) that may accumulate arsenic (Cui and Okayasu, 2008). This accumulation in the spleen alters the level and distribution of elements such as Fe, Cu and Zn in different rat organs, such as the kidney and brain (Rubatto Birri et al., 2010; Rubio et al., 2008). Other species also show effects of As on the tissue content of metals (Abdel-Gawad et al., 2016; García-Sevillano et al., 2013).

Therefore, our aim was to analyse arsenic-induced effects on the redox and metal homeostasis of the spleen and its cells, as possible mechanisms of immune impairment. To accomplish this, we had to assess the spatial distribution of metals in the spleen after sixty days of exposure to sodium arsenite in drinking water (100 ppm), using X-ray fluorescence analysis (XRF), which is non-destructive and performs multi-element analysis without prior preparation (Rubatto Birri et al., 2010; Rubio et al., 2008).

2. Materials and methods

2.1. Chemicals and supplies

Sodium arsenite ($NaAsO_2$) was purchased from Anedra (Argentina), rodent food from GEPSA Grupo Pilar SA (Argentina), and other reagents, standard reference materials and general chemicals from Sigma-Aldrich Co. (USA). Governmentally-certified water (As <10 μg/L) was supplied by Aguas Cordobesas SA (Argentina). The possibility of food contamination with arsenic was assessed using conventional wavelength dispersive XRF spectrometry (with levels below the detection limit −1 μg/g-).

The standard reference material 1577c (National Institute of Standards & Technology, USA) and TORT-2 (lobster hepatopancreas reference material for trace metals with 21 mg/kg of As, Institute for National Measurement Standards, Canada) were used for SR-μXRF (micro X-ray fluorescence spectrometry using Synchrotron radiation). TraceCERT® standards in the cellulose matrix (iron −Fe-, copper −Cu-, zinc −Zn-, arsenic −As-; with 1 g/L As in nitric acid, Sigma-Aldrich Co., USA) were used for EDXRF (energy dispersive X-ray fluorescence spectrometry).

2.2. Animal model and samples

Optimal experimental conditions (dose, time, species, sex, age) for developing an animal model of chronic arsenic poisoning to emulate human exposure were previously published (Rubatto Birri et al., 2010). These conditions had no effect on feeding, body weight, organ weights (brain, spleen, kidneys, heart, liver, pancreas, and testes), behaviour, and survival. This model is according to the high chronic exposure to As of 4.5 million people throughout their lives in Latin America (McClintock et al., 2012). Animals (2-month-old Wistar male rats) were divided into two equal groups of eight. One group received drinking water *ad libitum* containing 100 ppm of sodium arsenite (equivalent to 57.7 ppm of As) for 60 days (≈5.5% of lifespan). The control group received drinking water without As (0 ppm) under the same conditions. Water was changed daily. The animals were sacrificed the next day by isoflurane inhalation, with all procedures in accordance with ethical concerns and good laboratory practices (86/609/CEE). After autopsy, spleens were obtained, cut into 0.5 mm slides and lyophilised for X-ray-based techniques. Spleen fractions were used to isolate splenocytes (from C and As-treated animals) for other assays according to a reported procedure (Soria et al., 2014), with cellular viability (>95%) being confirmed by trypan blue exclusion.

2.3. Splenocyte culture and in vitro assay

In order to confirm the effects of arsenic on spleen parenchyma cells, splenocytes from unexposed rats (200 μL with 1000 cells/μL in 96-well plates) were treated *in vitro* with 0 or 7.5 μg/mL of As (corresponding to As concentrations found by SR-μXRF in the white pulp of exposed spleens, with other authors supporting similar values in blood) (Nandi et al., 2008), for 72 h in accordance with a previous study of dose-response effects on cells (Soria et al., 2014), by using isolated cells maintained at 37 °C in a 5% CO_2 atmosphere (1000 cells per 1 μL of RPMI-1640 medium with 10% foetal bovine serum and 100 μM ciprofloxacin). Additionally, subsets were co-treated with 5 μg/mL of concanavalin A or 5 μg/mL of lipopolysaccharide, to evaluate the effects of arsenic on the mitogenic response of splenocytes (Soria et al., 2014).

2.4. Markers of redox response

The specific activity of three redox-related enzymes was measured in mechanically homogenised splenocyte cultures from all experimental groups by colourimetric methods, and protein content was determined by the Bradford method:

γ-Glutamyltranspeptidase (GGT, EC 2.3.2.2): 100 mM pH 8.5 Tris buffer with substrates (2.9 mM L-γ-glutamyl-3-carboxy-4-nitroanilide 100 mM glycylglycine) was added to the sample at a 1:10 ratio. Results were calculated as follows: ΔA/min (average difference of absorbance at 405 nm per minute) × 1158 (constant)/cellular proteins, to be expressed as pNA nmol/min/mg, under conditions of initial velocity and linearity (Quiroga et al., 2010).

Nitric oxide synthase (NOS, EC 1.14.13.39): L-citrulline formation was assayed by mixing samples (5% trichloroacetic acid-deproteinised supernatant) with chromogenic solution (1 part 0.5% diacetylmonoxime plus 0.01% thiosemicarbazide, 2 parts 0.025% $FeCl_3$ in a solution of 25% sulphuric acid and 20% phosphoric acid) at a 0.1:3 ratio. After heating for 5 min (96 °C) and cooling, 530-nm absorbance was recorded to calculate L-citrulline μmol/mg using a standard curve (Boyde and Rahmatullah, 1980).

Peroxidase (PO, EC 1.11.2.2): Chromogenic solution (ethanol 1% *O*-phenyldiamine (OPD) stable for 4 h), 0.05% H_2O_2 and sample were mixed (0.1/4.9/5, respectively) at 25 °C in darkness. The reaction was measured at 570 nm after 5-min incubation (linear kinetics up to 15 min). The ΔA/min was converted to OPD μmol/min/mg prot by multiplying by 0.0111 (derived from the extinction molar coefficient 9.9 cm^{-1} mM^{-1} in 110 μL) (Bovaird et al., 1982).

2.5. Energy dispersive X-ray fluorescence (EDXRF) spectrometry

Sample elemental characterisations were carried out at the Spanish Institute of Earth Sciences "Jaume Almera". Briefly, mapping of X-ray fluorescence intensities in fine sections was made using an EDXRF Fischer XDV-SD spectrometer with a 50 keV tungsten-anode X-ray tube as the radiation source (50 W), a 0.3 mm diameter collimated excitation beam and a titanium filter. Each sample was positioned in a motorised plate stage with a three-axis (x,y,z) remote-controlled stage. A video microscope (45× magnifications) was used to locate the incoming beam. Fluorescence spectra were recorded with a Si(Pin) detector in air in the horizontal plane at 45° from the incident beam to minimise scattering. Elemental data were obtained by measuring X-ray fluorescence intensity of Kα spectral lines in red and white pulps (slices: 500 μm thick). The counting live-time for each pixel was 100 s/step and the step size was 0.3 mm, according to red-white pulp distribution in rat lyophilised spleen. Analysis of X-ray spectra by characteristic Kα spectral lines of elements was used for calculations of net peak, area and mass concentrations by WinFTM® v.6.20 software (Helmut Fisher GmbH Co., KG). Samples were analysed both by fundamental parameters, using generic organic matter Z matrix effective correction, and by empirical calibration. In the latter, cellulose standards spiked with 5, 25, 40, 100, 500 and 1000 mg/kg of arsenic were used for the instrumental calibration. Accuracy of the method was tested on standard reference materials. The results were expressed as μg/g of dry tissue.

2.6. Micro X-ray fluorescence spectrometry using synchrotron radiation (SR-μXRF)

Micro X-ray fluorescent intensity values were obtained at the Brazilian Synchrotron Light Laboratory. The energy of the electron bunch inside the storage ring reached 1.37 GeV. A dipole bending magnet (1.65-T magnetic field intensity) accelerates the electron bunch, which emits a photon spectrum with a critical energy of 2.08 keV. Photons were guided into the DO9 B beamline, where the XRF setup was placed. A spatial resolution of 30 μm × 30 μm was obtained by focusing the beam with a tapered glass monocapillary. Then, measurements were performed by exciting samples with a white SR beam (acquirement time, 100 s/step), with resulting spectra being analysed with specific mathematical algorithms (AXIL: analysis of X-ray spectra by iterative least squares). Each sample was positioned in the image plane within an accuracy of 0.5 mm with a 3 axis (x,y,z) remote-controlled stage. A video microscope (500× magnifications) was used to spot the pixels of reference precisely in the incoming microbeam. XRF measurements were performed using a standard geometry (45°–45°). The excitation beam was collimated by an orthogonal collimator. In this way, pixels were obtained by keeping a high flux of photons on the sample. The lens was mounted on a precision remote control stage which enabled its correct alignment. Fluorescence spectra were recorded with a Si(Li) detector of 165 eV FWHM at 5.9 keV in air atmosphere. This was set in the horizontal plane at 90° to the incident beam to minimise scattering. Kα X-ray fluorescence intensity scanning was performed. The area selected for two-dimensional scanning (x,y) was a representative part of the spleen covering nearly 1/4 of the total sample, approximately, containing white and red pulps. For 2-D graphics, a transect line of several points was obtained by measuring Kα X-ray fluorescence intensity (slices: 100 μm thick). The counting live-time for each pixel was 100 s/step and the step size was 30 μm. Using these counting live-times, data errors by SR-μXRF methodologies were <0.1% (Rubatto Birri et al., 2010).

2.7. Confirmation of immune compromise

Rats infected with *Corynebacterium kutscheri* (n = 8 diagnosed by microagglutination, survey code E01-09R, Laboratory Animals Department, UNLP, Argentina) were exposed to drinking water without and with sodium arsenite (100 ppm). This infection is lethally aggravated in immunodeficient rodents (National Research Council (US) Committee on Immunologically Compromised Rodents, 1989; Percy and Barthold, 2007). Survival of both groups over 60 d was compared by the Kaplan-Meier method followed by the log-rank test.

2.8. Statistical analysis

All analytical tests were performed using the InfoStat v2012 software, with $p < 0.05$ considered significant. Data were expressed as mean ± standard error (SE). T-test was used to compare differences between treatments. Path analysis was used to evaluate variable interactions. This statistical method is a case of structural equation modelling used to describe directed dependencies among variables by causality-focused multiple regression (Genser et al., 2007). It discriminates different routes between variables (direct and indirect effects, via covariables) by assigning their coefficients, which are used to algebraically compute total correlation. Thus, main direct routes can be identified and presented by a flow-chart (MacKinnon et al., 2007).

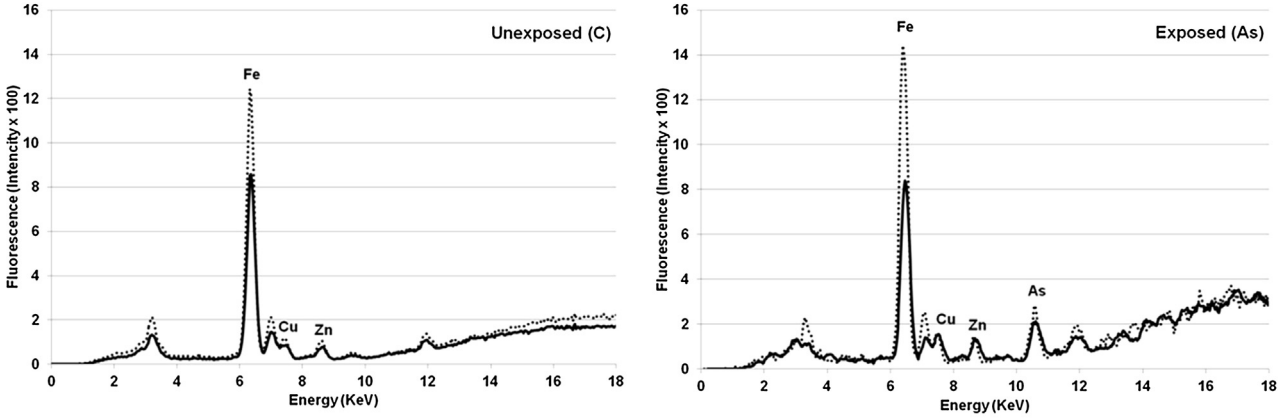

Fig. 1. EDXRF spectrograms of spleens from unexposed control and *in vivo* exposed rat (100 ppm of sodium arsenite, 2 months). Images are representative of five 100-s measurements (dashed line: red pulp, solid line: white pulp).

Partial least squares regression (PLS), computed by singular value decomposition, is a multivariate statistical method to generalise and combine principal component analysis and linear regression analysis, in order to predict a set of dependent variables from a set of predictors. This method informed the standardised correlations, which were plotted with variables represented as lines with a common central point. Line length indicated the relative intensity of variables, with correlation being shown as grades of line separation and direction (i.e. $<90°$ = positive, $90°$ = null, $>90°$ = negative) (Sæbø et al., 2008).

3. Results

The EDXRF analysis showed arsenic accumulation in white and red pulps ($p < 0.005$). Zn and Cu were also detected in both pulps, while Fe was higher in the red pulp ($p < 0.01$) (Fig. 1).

The SR-μXRF analysis (Fig. 2) confirmed EDXRF outcomes, although its high resolution coupled with lower relative error displayed lower values. Additional discriminations were found after arsenic exposure (Table 1). Arsenic increased Fe and Zn, but decreased Cu ($p < 0.01$), depending on location (pulps). Also, K, Ca and Mn were able to be measured by SR-μXRF. These changes

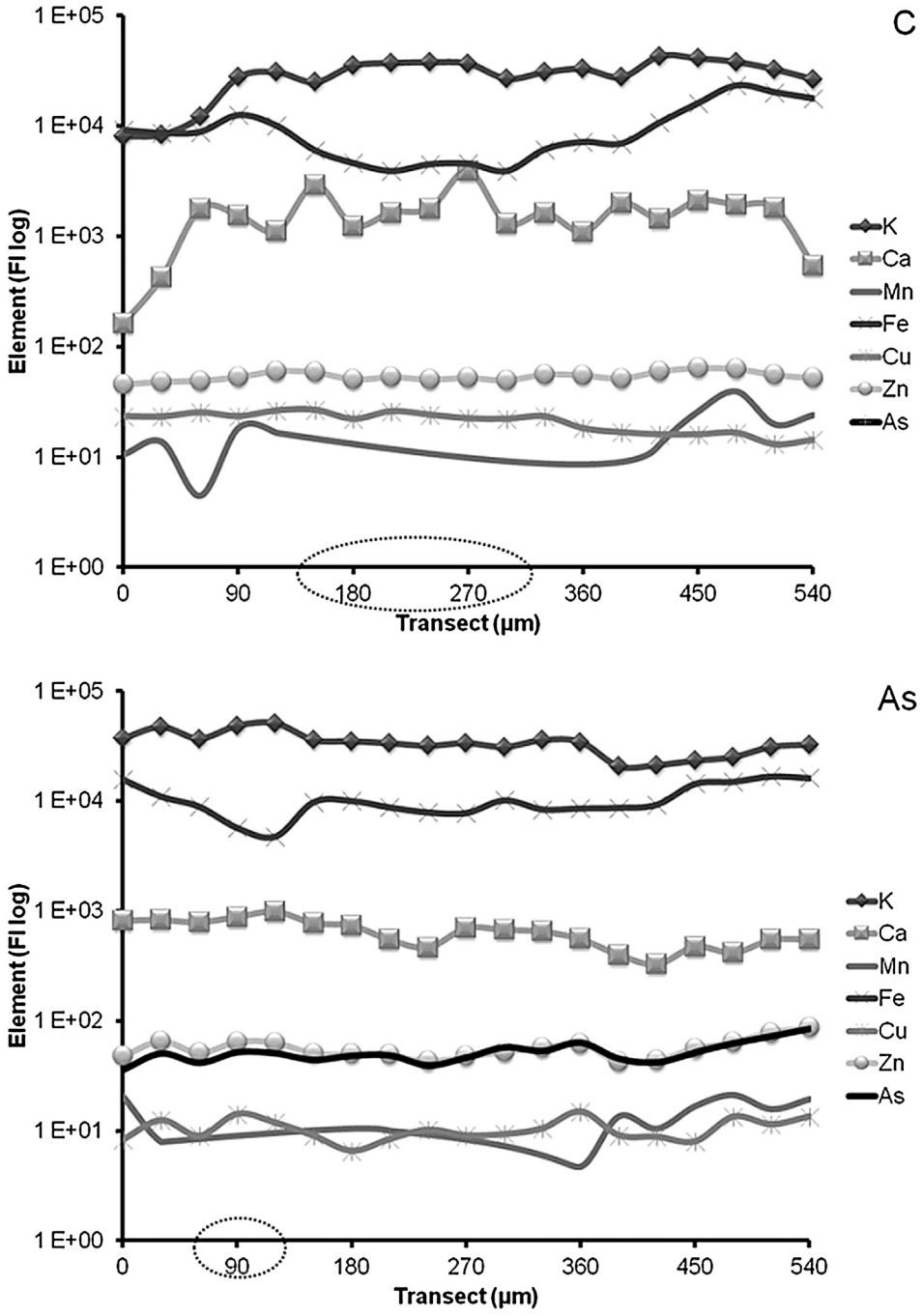

Fig. 2. Spleen SR-μXRF (Fl: fluorescence intensity, logarithmic scale) after 2-months treatment (C: control, As: 100 ppm of sodium arsenite). Graphics are representative spleen transects of multi-sampling measurements, with circled X-axis marks indicating white pulp.

Table 1
Technical outcomes of elemental content in spleen of male rats according to exposure (exposed or unexposed to 100 ppm of sodium arsenite).

METHOD	PULP	Fe		Cu	
		Unexposed	Exposed	Unexposed	Exposed
EDXRF	Red	2040.56 ± 62.58	1833.40 ± 58.66	2.50 ± 0.75	2.53 ± 0.37
	White	*1454.32 ± 176.48*	*1488.73 ± 72.38*	1.99 ± 0.29	2.06 ± 0.64
SR-μXRF	Red	758.30 ± 89.89	1167.76 ± 140.46	1.74 ± 0.17	1.66 ± 0.17
	White	*298.47 ± 24.85*	669.56 ± 85.32	2.03 ± 0.07	**1.23 ± 0.09**

METHOD	PULP	Zn		As	
		Unexposed	Exposed	Unexposed	Exposed
EDXRF	Red	49.64 ± 3.10	48.84 ± 2.20	0.38 ± 0.03	**147.72 ± 6.01**
	White	37.72 ± 2.65	44.75 ± 2.88	0.35 ± 0.04	***119.84 ± 3.48***
SR-μXRF	Red	11.32 ± 0.33	**15.36 ± 0.91**	0.03 ± 0.03	**29.45 ± 1.76**
	White	*9.89 ± 0.19*	***13.33 ± 0.94***	0.10 ± 0.05	**26.63 ± 2.21**

Bold indicates statistical differences with respect to unexposed controls, while *italic* indicates differences between pulps ($p < 0.01$). Units: mean ± SE ($n = 8$) as μg/g of dry tissue.

showed spatial correlations in 540-μm spleen transects in Fig. 2 and analysed in Fig. 3. Although the levels of As in control spleens close to the detection limit did not show a visible As line in C of Fig. 2, these levels allowed correlations to be calculated. Arsenic increase was inversely correlated with Cu and Ca, and positively with Zn. These As-related metal disturbances were induced by direct effects, with the Cu and Ca association being indirect and mediated by As. On the other hand, Fe was directly correlated with Zn and Mn, and inversely with Cu ($p < 0.05$), while Zn and K were directly correlated ($p < 0.02$).

In vivo arsenic exposure caused GGT reduction and PO induction, with no effect on NOS in splenocytes ($p < 0.05$) (Fig. 4), and these outcomes were confirmed in splenocytes exposed to As *in vitro* ($p < 0.05$). Cells treated with lipopolysaccharide and exposed to As showed induction of NOS and PO, with no effect on GGT ($p < 0.05$). Cells treated with concanavalin A showed reduction of GGT and NOS, but PO induction ($p < 0.05$) (Fig. 5). The effect on GGT of *in vivo* exposure to As was also seen *in vitro* in splenocytes treated with concanavalin A. The lack of NOS response *in vivo* was because splenocytes included two different types (that respond to concanavalin A or lipopolysaccharide), which showed differential responses to As. On the other hand, PO induction was always found.

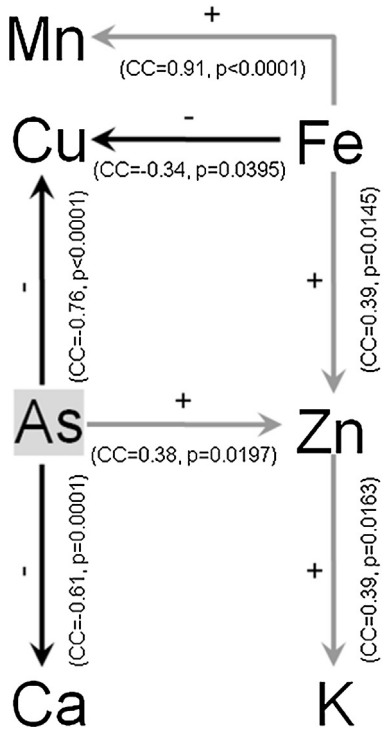

Fig. 3. Elemental directed associations in SR-μXRF spatial distributions, with positive (grey arrows, +) or negative (black arrows, −) outcomes (CC: correlation coefficient), assessed by path analysis at $p < 0.05$.

Statistical effects of the tissue concentration of arsenic were found on the enzyme activity of peroxidase, nitric oxide synthase (positive correlation), and γ-glutamyltranspeptidase (negative

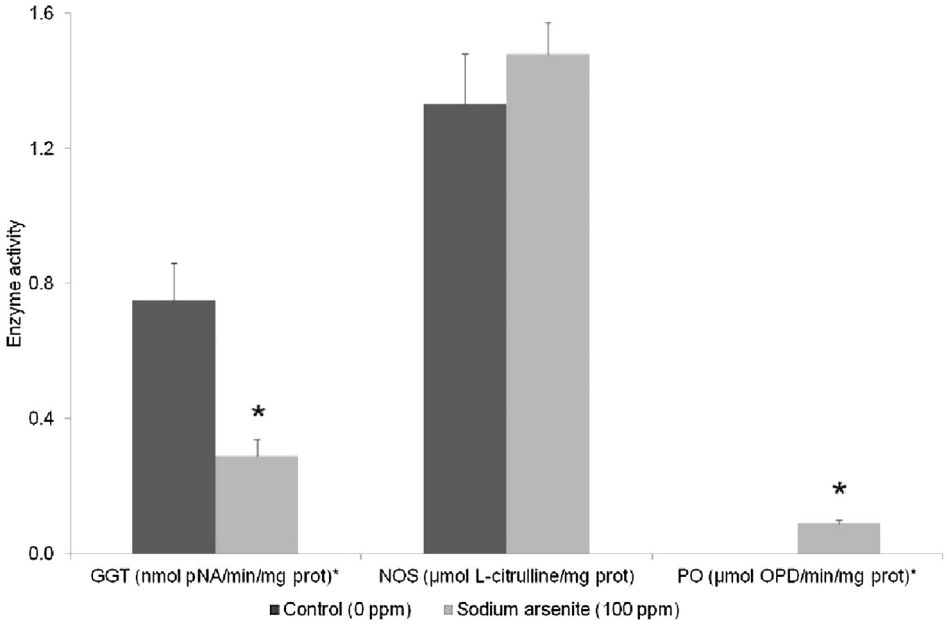

Fig. 4. Enzyme activity of γ-glutamyltranspeptidase (GGT), nitric oxide synthase (NOS) and peroxidase (PO), in splenocytes exposed *in vivo*. * Significant differences at $p < 0.05$ (mean ± SE, $n = 8$), with respect to controls.

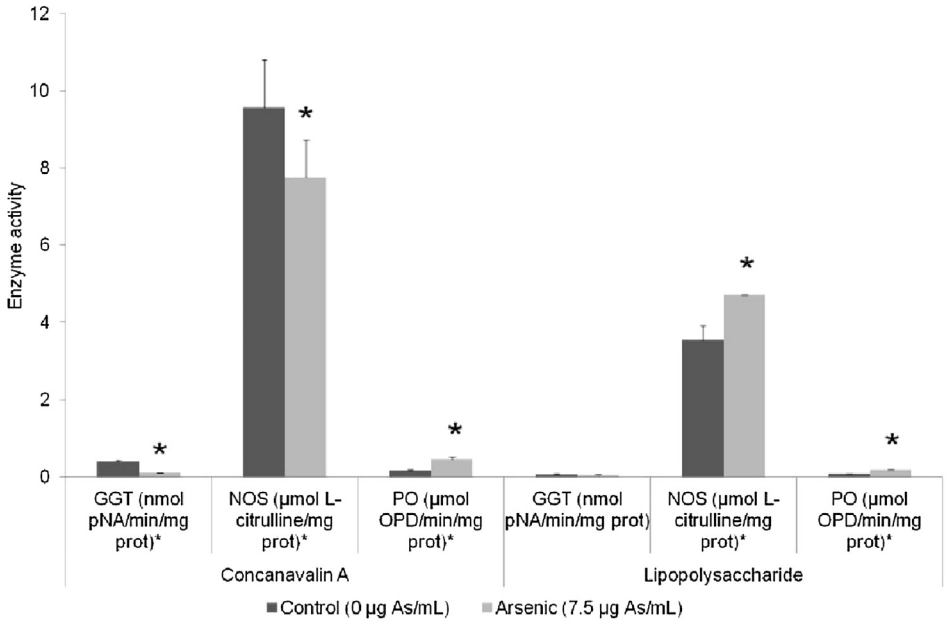

Fig. 5. Enzyme activity of γ-glutamyltranspeptidase (GGT), nitric oxide synthase (NOS) and peroxidase (PO), in mitogen-stimulated splenocytes exposed *in vitro*. * Significant differences at $p < 0.05$ (mean ± SE, n = 8), with respect to controls.

correlation) in the white pulp of spleen. Arsenic-related reductions of the tissue concentration of calcium and particularly copper were related in these responses. Effects on enzymes and related metals were poorly associated in the red pulp, where Fe, Mn, and Zn were associated. K showed poor involvement. Given that PLS associates elements, enzymes and spleen pulps, variables are positioned in accordance with their location (Fig. 6).

Immune impairment was confirmed. Exposure to sodium arsenite increased mortality, with all animals being dead after 40 days, a significant difference with respect to control rats

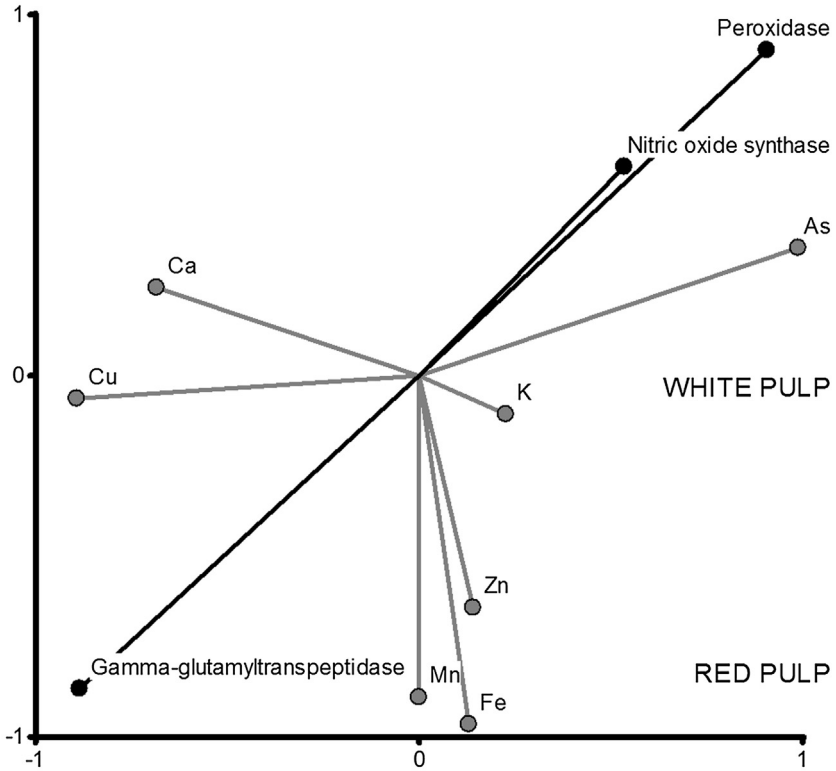

Fig. 6. Regression of partial least squares of variables analysed after *in vivo* exposure (0 −Control-, or 100 ppm of sodium arsenite), to plot relative intensity (length) and type of correlations (positive: similar direction, negative: opposite direction). Grey lines: Tissue concentration of elements taken as predictors from spleen pulps. Black lines: Activity of enzymes taken as responses.

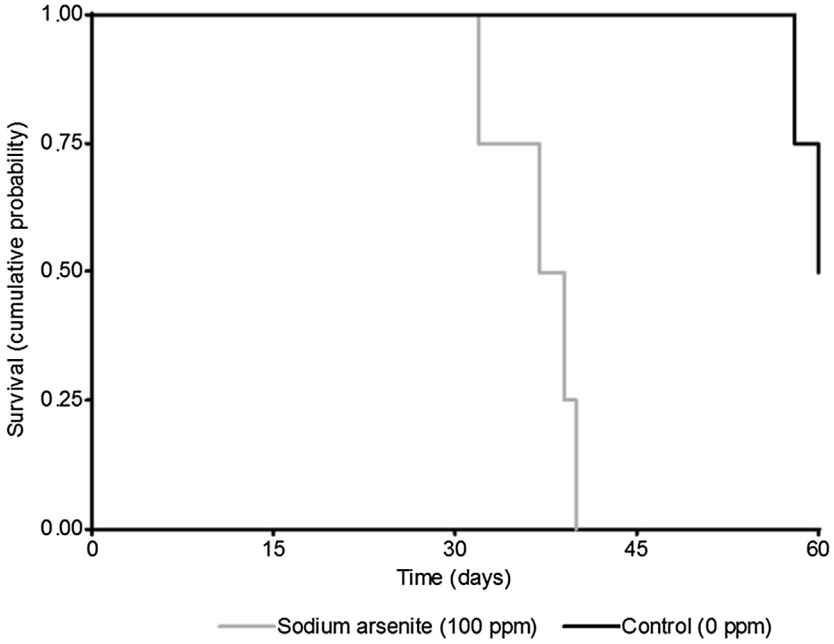

Fig. 7. Kaplan-Meier survival curves of rats infected with *C. kutscheri* and exposed to 0 (control) or 100 ppm of sodium arsenite (p = 0.0158).

(p = 0.0158, Fig. 7). All non-infected animals with or without As treatment survived out to 60 days.

4. Discussion

Arsenic incorporation results from the high oral bioavailability of its soluble salts in all mammals, with pharmacokinetic parameters in rats (e.g. fast absorption, slow clearance, erythrocyte affinity) promoting time-dependent bioaccumulation (Diacomanolis et al., 2014). The spleen thus accumulates circulating arsenic, which is distributed in both pulps with different cellular populations and tissue constitution. Our own data of SR-μXRF XANES (spectroscopy of X-ray absorption near edge structure) suggested inorganic trivalent arsenic (AsIII) and monomethyl arsenic (organic MMAsIII) as major species in spleen cells (Pérez et al., 2010; unpublished data). Since the dimethyl form (DMAsIII) is bound to rat haemoglobin (Lu et al., 2007), and pentavalent and methylthiol species are excreted via urine (Chen et al., 2016), other trivalent forms are retained in spleen.

EDXRF is a valuable tool to determine As bioaccumulation with good reproducibility. Its relative standard deviation (RSD) is 13.8% using the 0.3 mm collimator and 100 s. Additionally, its titanium filter reduces spectral noise to appropriately quantify peak areas. However, the fluorescent intensity of elements in samples is also affected (30.7% of mean), as is confirmed in cellulose standards using an aluminium filter. SR-μXRF provides high resolution and low RSD even with this filter. The thickness of slices used for each method (EDXRF: 500 μm vs. SR-μXRF: 100 μm) also explained the technical outcomes.

At high spatial resolution, arsenic accumulation modified metal content and distribution, with Fe and Fe-Cu-Zn interdependence playing central roles in metal homeostasis and lymphocyte development (Blaby-Haas and Merchant, 2014; Carpentieri et al., 1988; Gulec and Collins, 2014). Thus, path analysis showed the involvement of Fe in the distribution of Cu, Zn, and Mn. An iron increase is also found in pig spleen after dietary exposure to As (Wang et al., 2006). Fe and As were indirectly related, and ferritin and haemosiderin may be involved. Ferritin is induced to prevent apoptosis as antioxidant response that sequesters Fe in oxidative stress, which is triggered by arsenic (Huang et al., 2013). Also, haemosiderin accumulation is another As immunotoxic mechanism (Ghosh et al., 2007).

Copper levels in spleen regions were decreased by arsenic exposure, matching the total Cu reduction previously found (Wang et al., 2006). This effect depends on Cu redistribution outside the spleen in the model used, leading to renal accumulation of this metal (Rubatto Birri et al., 2010). Arsenic also impairs the endomembrane system involved in metal homeostasis and the metallothionein-related response (Blaby-Haas and Merchant, 2014; Grasso et al., 2011), which regulates Cu and Zn levels (Garla et al., 2013). The distribution of Zn is also a response to counteract As toxicity (Kumar et al., 2010), with both elements reciprocally affecting their organic fates (Kumar et al., 2011). On the other hand, calcium reduction by arsenic can be related to metabolic disruption, mitochondrial targeting and the compromise of Ca signalling (Hsu et al., 2012; Miltonprabu and Sumedha, 2014). Therefore, essential metal supplementation is proposed to reverse As toxicity (Kumar et al., 2010; Srivastava et al., 2010), and to promote immunity (Carpentieri et al., 1988).

Given that spleens were haemolysed with stroma removed, splenocytes mostly include lymphocytes and some other mononuclear immune cells, which can be stimulated by different mitogens (Soria et al., 2014). These cells predominate in spleen white pulp, which showed the main metal disturbances induced by As accumulation. This was confirmed by PLS analysis, which also explained the metal effect on the redox enzymes, peroxidase, nitric oxide synthase and γ-glutamyltranspeptidase, with an important involvement of copper. Moreover, GGT, an enzyme related to lymphocyte viability and immune response (Carlisle et al., 2003), was reduced by arsenic, which can trigger oxidative stress. In this sense, PO induction matched the widespread capacity of arsenic to trigger peroxidation in biological systems (Sarath et al., 2014). Given the reduction of GGT activity and metal imbalance, peroxides can increase and be available to a PO reaction, which

is enhanced by glutathione depletion, redox stress and inflammation (Quiroz et al., 2015; Ramos Elizagaray and Soria, 2014; Reyes et al., 2005).

Regarding the redox enzymes, GGT was active in cells responding to concanavalin A, but not in cells treated with lipopolysaccharide, with arsenic impairing this response. Also, NOS was induced by concanavalin A and lipopolysaccharide, as expected (Walia et al., 2015). This induction was affected by arsenic in the first case, but it continued in the latter with a slight enhancement. T cells may therefore be the main target of arsenic toxicity, as concanavalin A and lipopolysaccharide are respectively T and B mitogens (Lozano-Ojalvo et al., 2016). Moreover, GGT is differentially expressed in T lymphocytes depending on their activation: absent in naive cells, high in active cells and intermediate in memory subsets (Carlisle et al., 2003), with their receptor and stimulation being dependent on GGT-related redox regulation (Reyes et al., 2005). Mechanistically, arsenic caused Cu deficiency which down-regulated glutathione-related pathways (Quiroz et al., 2015), with Zn being unable to restore the catalytic activity (Ahmad et al., 2013). Arsenic also disturbed Ca, which blocked T activation and GGT expression (Lee et al., 2015). This arsenic-related Ca reduction may additionally impair NOS induction (Huang et al., 2011). It is important to keep in mind that these metals can act directly in redox homeostasis (Zhong et al., 2014). Also, different isozymes of the enzymes evaluated can respond oppositely to arsenic (Sarath et al., 2014).

5. Conclusions

Taken together, our results indicate that arsenic impaired the spatial homeostasis of important biometals, such as Ca, Cu, Zn and Fe, in the spleen, with the corresponding compromise of enzyme responses of spleen cells, which supported the immunodeficiency induced by arsenic, depending on differential metal-related physiology and toxicological susceptibility of immunocytes, mainly T cells.

Conflict of interest

None.

Disclosure statement

Dr. Bongiovanni reports grants from Agencia Nacional de Promoción Científica y Tecnológica, during the conduct of the study.

Dr. Queralt reports grants from International Cancer Technology Transfer Fellowship, during the conduct of the study.

Acknowledgements

This work was supported by Agencia Nacional de Promoción Científica y Tecnológica [grant n° PICT-2013-0458, Argentina], Consejo Nacional de Investigaciones Científicas y Técnicas [grant n° PIP-02394, Argentina], Laboratório Nacional de Luz Síncrotron [grant n° D09B-15254, D09B-15256, D09B-XRF-11903, Brazil], International Cancer Technology Transfer Fellowship [contract n° NO2-CO-41101, Switzerland], Universidad Nacional del Comahue [grant n° 04-N025, Argentina], and Universidad Nacional de Córdoba [grant n° SECYT-162/2012, SECYT-203/2014, Argentina]. The funding sources had no involvement in the study design, data management or article writing and submission, and the authors declare they have no conflicts of interest.

Appendix A. Supplementary data

Supplementary data associated with this article can be found, in the online version, at http://dx.doi.org/10.1016/j.toxlet.2016.12.014.

References

Abdel-Gawad, M., Elsobky, E., Shalaby, M.M., Abd-Elhameed, M., Abdel-Rahim, M., Ali-El-Dein, B., 2016. Quantitative evaluation of heavy metals and trace elements in the urinary bladder: comparison between cancerous, adjacent non-cancerous and normal cadaveric tissue. Biol. Trace Element Res. 174, 280–286.
Ahmad, M., Wadaa, M.A.M., Farooq, M., Daghestani, M.H., Sami, A.S., 2013. Effectiveness of zinc in modulating perinatal effects of arsenic on the teratological effects in mice offspring. Biol. Res. 46, 131–138.
Biswas, D., Banerjee, M., Sen, G., Das, J.K., Banerjee, A., Sau, T.J., Pandit, S., Giri, A.K., Biswas, T., 2008. Mechanism of erythrocyte death in human population exposed to arsenic through drinking water. Toxicol. Appl. Pharmacol. 230, 57–66.
Blaby-Haas, C.E., Merchant, S.S., 2014. Lysosome-related organelles as mediators of metal homeostasis. J. Biol. Chem. 289, 28129–28136.
Bovaird, J.H., Ngo, T.T., Lenhoff, H.M., 1982. Optimizing the o-phenylenediamine assay for horseradish peroxidase: effects of phosphate and pH substrate and enzyme concentrations, and stopping reagents. Clin. Chem. 28, 2423–2426.
Boyde, T.R., Rahmatullah, M., 1980. Optimization of conditions for the colorimetric determination of citrulline, using diacetyl monoxime. Anal. Biochem. 107, 424–431.
Bundschuh, J., Litter, M.I., Parvez, F., Román-Ross, G., Nicolli, H.B., Jean, J., Liu, C., López, D., Armienta, M.A., Guilherme, L.R.G., Gómez Cuevas, A., Cornejo, L., Cumbal, L., Toujaguez, R., 2012. One century of arsenic exposure in Latin America: a review of history and occurrence from 14 countries. Sci. Total Environ. 429, 2–35.
Carlisle, M.L., King, M.R., Karp, D.R., 2003. Gamma-glutamyl transpeptidase activity alters the T cell response to oxidative stress and Fas-induced apoptosis. Int. Immunol. 15, 17–27.
Carpentieri, U., Myers, J., Daeschner, C.W., Haggard, M.E., 1988. Effects of iron, copper, zinc, calcium, and magnesium on human lymphocytes in culture. Biol. Trace Element Res. 16, 165–176.
Chakraborti, D., Nriagu, J.O., 2011. Arsenic: Occurrence in groundwater. Encyclopedia of Environmental Health. Elsevier B.V., Amsterdam, pp. 165–180.
Chen, B., Lu, X., Arnold, L.L., Cohen, S.M., Le, X.C., 2016. Identification of methylated dithioarsenicals in the urine of rats fed with sodium arsenite. Chem. Res. Toxicol. 29, 1480–1487.
Cui, X., Okayasu, R., 2008. Arsenic accumulation, elimination, and interaction with copper: zinc and manganese in liver and kidney of rats. Food Chem. Toxicol. 46, 3646–3650.
Diacomanolis, V., Noller, B.N., Ng, J.C., 2014. Bioavailability and pharmacokinetics of arsenic are influenced by the presence of cadmium. Chemosphere 112, 203–209.
García-Sevillano, M.A., Jara-Biedma, R., González-Fernández, M., García-Barrera, T., Gómez-Ariza, J.L., 2013. Metal interactions in mice under environmental stress. Biometals 26, 651–666.
Garla, R., Mohanty, B.P., Ganger, R., Sudarshan, M., Bansal, M.P., Garg, M.L., 2013. Metal stoichiometry of isolated and arsenic substituted metallothionein: PIXE and ESI–MS study. Biometals 26, 887–896.
Genser, B., Cooper, P.J., Yazdanbaksh, M., Barreto, M.L., Rodrigues, L.C., 2007. A guide to modern statistical analysis of immunological data. BMC. Immunol. 8, 27.
Ghosh, D., Datta, S., Bhattacharya, S., Mazumder, S., 2007. Long-term exposure to arsenic affects head kidney and impairs humoral immune responses of Clarias batrachus. Aquat. Toxicol. 81, 79–89.
Grasso, E.J., Bongiovanni, G.A., Pérez, R.D., Calderón, R.O., 2011. Pre-cancerous changes in urothelial endocytic vesicle leakage, fatty acid composition, and As and associated element concentrations after arsenic exposure. Toxicology 284, 26–33.
Gulec, S., Collins, J.F., 2014. Molecular mediators governing iron-copper interactions. Annu. Rev. Nutr. 34, 95–116.
Hong, Y., Song, K., Chung, J., 2014. Health effects of chronic arsenic exposure. J. Prev. Med. Public Health 47, 245–252.
Hsu, W.L., Tsai, M.H., Lin, M.W., Chiu, Y.C., Lu, J.H., Chang, C.H., 2012. Differential effects of arsenic on calcium signaling in primary keratinocytes and malignant (HSC-1) cells. Cell Calcium 52, 161–169.
Huang, Z., Hoffmann, F.W., Fay, J.D., Hashimoto, A.C., Chapagain, M.L., Kaufusi, P.H., Hoffmann, P.R., 2011. Stimulation of unprimed macrophages with immune complexes triggers a low output of nitric oxide by calcium-dependent neuronal nitric-oxide synthase. J. Biol. Chem. 287, 4492–4502.
Huang, B.W., Ray, P.D., Iwasaki, K., Tsuji, Y., 2013. Transcriptional regulation of the human ferritin gene by coordinated regulation of Nrf2 and protein arginine methyltransferases PRMT1 and PRMT4. FASEB J. 27, 3763–3774.
Jomova, K., Jenisova, Z., Feszterova, M., Baros, S., Liska, J., Hudecova, D., Rhodes, C.J., Valko, M., 2011. Arsenic: toxicity, oxidative stress and human disease. J. Appl. Toxicol. 31, 95–107.
Kumar, A., Malhotra, A., Nair, P., Garg, M.L., Dhawan, D.K., 2010. Protective role of zinc in ameliorating arsenic-induced oxidative stress and histological changes in rat liver. J. Environ. Pathol. Toxicol. Oncol. 29, 91–100.

Kumar, A., Nair, P., Malhotra, A., Majumdar, S., Garg, M.L., Dhawan, D.K., 2011. Altered uptake and biological half-lives of 65Zn on arsenic exposure – modulation by zinc treatment. Biol. Trace Elem. Res. 144, 1059–1068.
Lee, M.D., Bingham, K.N., Mitchell, T.Y., Meredith, J.L., Rawlings, J.S., 2015. Calcium mobilization is both required and sufficient for initiating chromatin decondensation during activation of peripheral T-cells. Mol. Immunol. 63, 540–549.
Lozano-Ojalvo, D., Molina, E., López-Fandiño, R., 2016. Hydrolysates of egg white proteins modulate T- and B-cell responses in mitogen-stimulated murine cells. Food Funct. 7, 1048–1056.
Lu, M., Wang, H., Li, X.F., Arnold, L.L., Cohen, S.M., Le, X.C., 2007. Binding of dimethylarsinous acid to cys-13alpha of rat hemoglobin is responsible for the retention of arsenic in rat blood. Chem. Res. Toxicol. 20, 27–37.
MacKinnon, D.P., Fairchild, A.J., Fritz, M.S., 2007. Mediation analysis. Annu. Rev. Psychol. 58, 593–614.
McClintock, T.R., Chen, Y., Bundschuh, J., Oliver, J.T., Navoni, J., Olmos, V., Lepori, E.V., Ahsan, H., Parvez, F., 2012. Arsenic exposure in Latin America Biomarkers, risk assessments and related health effects. Sci. Total Environ. 429, 76–91.
Miltonprabu, S., Sumedha, N.C., 2014. Arsenic-induced hepatic mitochondrial toxicity in rats and its amelioration by diallyl trisulfide. Toxicol. Mech. Methods 24, 124–135.
Nandi, D., Patra, R.C., Ranjan, R., Swarup, D., 2008. Role of co-administration of antioxidants in prevention of oxidative injury following sub-chronic exposure to arsenic in rats. Veterinarski Arhiv. 78, 113–121.
National Research Council (US) Committee on Immunologically Compromised Rodents, 1989. Immunodeficient Rodents: A Guide to Their Immunobiology, Husbandry, and Use. National Academies Press (US), Washington DC.
Pérez, C.A., Martins, B.S., Bongiovanni, G.A., 2010. Chemical Speciation of Bioaccumulated Arsenic by SR-TXRF-XANES LNLS Activity Report. , pp. 1829.
Paul, S., Das, N., Bhattacharjee, P., Banerjee, M., Das, J.K., Sarma, N., Sarkar, A., Bandyopadhyay, A.K., Sau, T.J., Basu, S., Banerjee, S., Majumder, P., Giri, A.K., 2013. Arsenic-induced toxicity and carcinogenicity: a two-wave cross-sectional study in arsenicosis individuals in West Bengal, India. J. Expo. Sci. Environ. Epidemiol. 23, 156–162.
Percy, D.H., Barthold, S.W., 2007. Pathology of Laboratory Rodents and Rabbits, third ed. Blackwell Publishing Professional, Ames.
Quiroga, A., Quiroga, P.L., Martínez, E., Soria, E.A., Valentich, M.A., 2010. Anti-breast cancer activity of curcumin on the human oxidation-resistant cells ZR-75-1 with gamma-glutamyltranspeptidase inhibition. J. Exp. Ther. Oncol. 8, 261–266.
Quiroz, N., Rivas, N., del Pozo, T., Burkhead, J., Suazo, M., González, M., Latorre, M., 2015. Transcriptional activation of glutathione pathways and role of glucose homeostasis during copper imbalance. Biometals 28, 321–328.
Ramos Elizagaray, S.I., Soria, E.A., 2014. Arsenic immunotoxicity and immunomodulation by phytochemicals: potential relations to develop chemopreventive approaches. Recent Pat. Inflamm. Allergy Drug Discov. 8, 92–103.
Ray, P.D., Yosim, A., Fry, R.C., 2014. Incorporating epigenetic data into the risk assessment process for the toxic metals arsenic, cadmium, chromium, lead, and mercury: strategies and challenges. Front. Genet. 5, 201.
Reyes, B.M.R., Danese, S., Sans, M., Fiocchi, C., Levine, A.D., 2005. Redox equilibrium in mucosal T cells tunes the intestinal TCR signaling threshold. J. Immunol. 175, 2158–2166.
Rubatto Birri, P.N., Pérez, R.D., Cremonezzi, D., Pérez, C.A., Rubio, M., Bongiovanni, G. A., 2010. Association between As and Cu renal cortex accumulation and physiological and histological alterations after chronic arsenic intake. Environ. Res. 110, 417–423.
Rubio, M., Perez, R.D., Perez, C.A., Eynard, A.R., Bongiovanni, G.A., 2008. Synchrotron microscopic X-ray fluorescence analysis of the effects of chronic arsenic exposure in rat brain. Radiat. Phys. Chem. 77, 1–8.
Sæbø, S., Almøy, T., Flatberg, A., Aastveit, A.H., Martens, H., 2008. LPLS-regression: a method for prediction and classification under the influence of background information on predictor variables. Chemometr. Intell. Lab. Syst. 91, 121–132.
Sarath, T.S., Waghe, P., Gupta, P., Choudhury, S., Kannan, K., Pillai, A.H., Harikumar, S. K., Mishra, S.K., Sarkar, S.N., 2014. Atorvastatin ameliorates arsenic-induced hypertension and enhancement of vascular redox signaling in rats. Toxicol. Appl. Pharmacol. 280, 443–454.
Schulz, H., Nagymajtényi, L., Institoris, L., Papp, A., Siroki, O., 2002. A study on behavioral, neurotoxicological, and immunotoxicological effects of subchronic arsenic treatment in rats. J. Toxicol. Environ. Health Part A 65, 1181–1193.
Sharma, B., Singh, S., Siddiqi, N.J., 2014. Biomedical implications of heavy metals induced imbalances in redox systems. BioMed. Res. Int. 2014, 640754.
Soria, E.A., Quiroga, P.L., Albrecht, C., Ramos Elizagaray, S.I., Cantero, J.J., Bongiovanni, G.A., 2014. Development of an antioxidant phytoextract of Lantana grisebachii with lymphoprotective activity against in vitro arsenic toxicity. Adv. Pharmacol. Sci. 416761.
Srivastava, D., Subramanian, R., Madamwar, D., Flora, S., 2010. Protective effects of selenium, calcium, and magnesium against arsenic-induced oxidative stress in male rats. Arh. Hig. Rada. Toksikol. 61, 153–159.
Tarantino, G., Scalera, A., Finelli, C., 2013. Liver-spleen axis Intersection between immunity, infections and metabolism. World J. Gastroenterol. 19, 3534–3542.
Ullah, N., Khan, M.F., Jan, S.U., Mukhtiar, M., Khan, H., Rehman, A., 2015. Study of the effect of inorganic and organic complexes of arsenic metal on the status of GSH in T cells and B cells of blood. Pak. J. Pharm. Sci. 28, 457–464.
Walia, V., Kumar, R., Mitra, A., 2015. Lipopolysaccharide and concanavalin A differentially induce the expression of immune response genes in caprine monocyte derived macrophages. Anim. Biotechnol. 26, 298–303.
Wang, L., Xu, Z.R., Jia, X.Y., Han, X.Y., 2006. Effects of dietary arsenic levels on serum parameters and trace mineral retentions in growing and finishing pigs. Biol. Trace Elem. Res. 113, 155–164.
Zhong, L., Wang, L., Xu, L., Liu, Q., Jiang, L., Zhi, Y., Lu, W., Zhou, P., 2014. The role of NOS-mediated ROS accumulation in an early phase Cu-induced acute cytotoxicity in MCF-7 cells. Biometals 28, 113–122.